

Generic real-time uniform K-space sampling method for high-speed swept-Source optical coherence tomography

Jiefeng Xi, Li Huo, Jiasong Li and Xingde Li*

Department of Biomedical Engineering, Johns Hopkins University, 720 Rutland Avenue, Baltimore, MD 21205, USA
*xingde@jhu.edu

Abstract: We developed a universal, real-time uniform K-space sampling (Rt-UKSS) method for high-speed swept-source optical coherence tomography (SS-OCT). An external clock uniform in K-space was generated. The clock was synchronized with the zero-crossing time of an interferometric calibration signal and used as triggers for a high-speed data acquisition system in a point-by-point fashion, hence enabling uniform data sampling in K-space. Different from the numerical calibration algorithm commonly used in an SS-OCT system, the method reported here does not require over-sampling, thus greatly reducing the demand for digitization, data processing and storage speed. The Rt-UKSS method is adaptive and applicable to a generic SS-OCT system of a wide range of A-scan rates without special adjustment. We successfully implemented the Rt-UKSS method in an SS-OCT system based on a Fourier-domain mode-locked laser (FDML) of a 40-kHz scanning rate. Real-time imaging of biological tissues using such a system was demonstrated with a measured axial resolution of 9.3 μm and detection sensitivity greater than 120dB.

©2010 Optical Society of America

OCIS codes: (110.4500) Optical coherence tomography; (170.3880) Medical and biological imaging

References and Links

1. M. A. Choma, M. V. Sarunic, C. H. Yang, and J. A. Izatt, "Sensitivity advantage of swept source and Fourier domain optical coherence tomography," *Opt. Express* **11**(18), 2183–2189 (2003).
 2. J. F. de Boer, B. Cense, B. H. Park, M. C. Pierce, G. J. Tearney, and B. E. Bouma, "Improved signal-to-noise ratio in spectral-domain compared with time-domain optical coherence tomography," *Opt. Lett.* **28**(21), 2067–2069 (2003).
 3. R. Leitgeb, C. K. Hitzenberger, and A. F. Fercher, "Performance of fourier domain vs. time domain optical coherence tomography," *Opt. Express* **11**(8), 889–894 (2003).
 4. S. R. Chinn, E. A. Swanson, and J. G. Fujimoto, "Optical coherence tomography using a frequency-tunable optical source," *Opt. Lett.* **22**(5), 340–342 (1997).
 5. A. F. Fercher, C. K. Hitzenberger, G. Kamp, and S. Y. Elzaiat, "Measurement of Intraocular Distances by Backscattering Spectral Interferometry," *Opt. Commun.* **117**(1-2), 43–48 (1995).
 6. R. Huber, M. Wojtkowski, and J. G. Fujimoto, "Fourier Domain Mode Locking (FDML): A new laser operating regime and applications for optical coherence tomography," *Opt. Express* **14**(8), 3225–3237 (2006).
 7. B. Potsaid, I. Gorczynska, V. J. Srinivasan, Y. L. Chen, J. Jiang, A. Cable, and J. G. Fujimoto, "Ultra-high speed spectral / Fourier domain OCT ophthalmic imaging at 70,000 to 312,500 axial scans per second," *Opt. Express* **16**(19), 15149–15169 (2008).
 8. R. Huber, M. Wojtkowski, K. Taira, J. G. Fujimoto, and K. Hsu, "Amplified, frequency swept lasers for frequency domain reflectometry and OCT imaging: design and scaling principles," *Opt. Express* **13**(9), 3513–3528 (2005).
 9. R. Huber, M. Wojtkowski, J. G. Fujimoto, J. Y. Jiang, and A. E. Cable, "Three-dimensional and C-mode OCT imaging with a compact, frequency swept laser source at 1300 nm," *Opt. Express* **13**(26), 10523–10538 (2005).
 10. C. M. Eigenwillig, B. R. Biedermann, G. Palte, and R. Huber, "K-space linear Fourier domain mode locked laser and applications for optical coherence tomography," *Opt. Express* **16**(12), 8916–8937 (2008).
-

1. Introduction

The recently developed Fourier-domain OCT technology (FD-OCT) has led to substantial improvements on A-scan rate and detection sensitivity over the conventional time-domain technologies [1–3]. Two approaches have been developed to deploy the Fourier-domain techniques: encoding the spectral information either in space with a dispersive component (e.g. a grating) and a CW broadband light source (spectral-domain OCT) or in time with a frequency scanning light source (swept-source OCT) [4–7]. Between these two approaches, swept-source OCT (SS-OCT) is generally chosen when imaging highly scattering epithelial tissues such as the esophagus, colon and aorta etc., at longer wavelengths (i.e. above 1 μm) where commercial high-speed CCD or CMOS line cameras of an adequate number of pixels for spectral-domain OCT are still lacking and/or costly.

Since its first demonstration at the wavelength of 1.3 μm , Fourier-domain mode-locked laser (FDML) has become the most convenient and powerful source for SS-OCT with an excellent combination of imaging speed, instantaneous coherence length, and spectral width among the frequency-swept laser sources [8,9]. Uninterrupted real-time imaging with a rapidly sweeping FDML requires high-speed analog-to-digital conversion, data processing, display and storage. Normally, a sinusoidal drive waveform is used to drive a fiber-optic Fabry-Perot tunable filter (FFP-TF) for wavelength sweeping and the response of the FFP-TF is nonlinear and hysteretic. Therefore, the OCT fringe signal that is typically digitized with a uniform time interval results in a nonuniform sample distribution in K-space. For real-time processing (which involves fast Fourier transform) and display, resampling or numerical calibration is required to convert the time-uniform OCT fringe data to a K-space uniform set prior to Fourier transform. There are several challenges associated with the numerical calibration procedure: (1) It slows down the overall data processing speed; (2) The OCT fringe signal needs to be digitized with sufficient density (e.g. at least 4-5 points per fringe) in order to perform accurate calibration, which increases the load of signal digitization, data transfer and storage; and (3) Since the calibration data is generally digitized only at a few time points during imaging, the numerical calibration methods can thus be sensitive to errors associated with any fluctuation in wavelength sweeping. Recently a light source with linear k-space sweeping has been successfully demonstrated; however this approach requires a pre-calculated and non-sinusoidal synthetic drive waveform, which is FFP-TF device specific and varies with sweeping frequency [10]. One potential solution to overcome the non-uniform K-space sampling issue and the associated problems mentioned above is to develop a generic, real-time uniform K-space sampling (Rt-UKSS) method. Although a similar concept was demonstrated with a conventional low-speed wavelength-swept laser (e.g. Micron Optics SS225 at 5 kHz), it has been challenging to implement a uniform K-sampling method for mainstream high-speed SS-OCT systems with a wavelength sweeping rate at least several tens kHz. In this paper, we present a new hardware-based Rt-UKSS method, which is implemented by designing and generating an external clock to provide point-by-point triggers with uniform spatial frequency spacing (in K-space) for the digitizer. This method relaxes the demands for data digitization, transfer, processing and storage speed by at least 2.5 folds, and thus it affords to handle an ~ 2.5 times higher A-scan rate for a given data acquisition system. This method is robust, adaptive, and applicable to a generic SS-OCT system as long as the scanning rate is within the frequency range of the external clock circuitry. In addition, this method is insensitive to the instability of the swept source such as the drift of the laser spectrum or wavelength sweeping drive waveform, and hence avoids any potential misalignment of the calibration signal with the real-time OCT fringe signal. Moreover, the new method can also handle a broader wavelength sweeping range since oversampling of the OCT fringe data is no longer required. Thus a light source of a broader spectrum bandwidth can be used in an SS-OCT system to achieve a higher axial resolution. This new method has been successfully implemented in a 40-kHz FDML-based SS OCT system which has measured detection sensitivity greater than 120dB and an axial resolution of 9.3 μm in air.

The performance of the new method was demonstrated by real-time imaging of biological tissues.

2. Experimental methods

2.1 Hardware-based real-time uniform K -space sampling approach

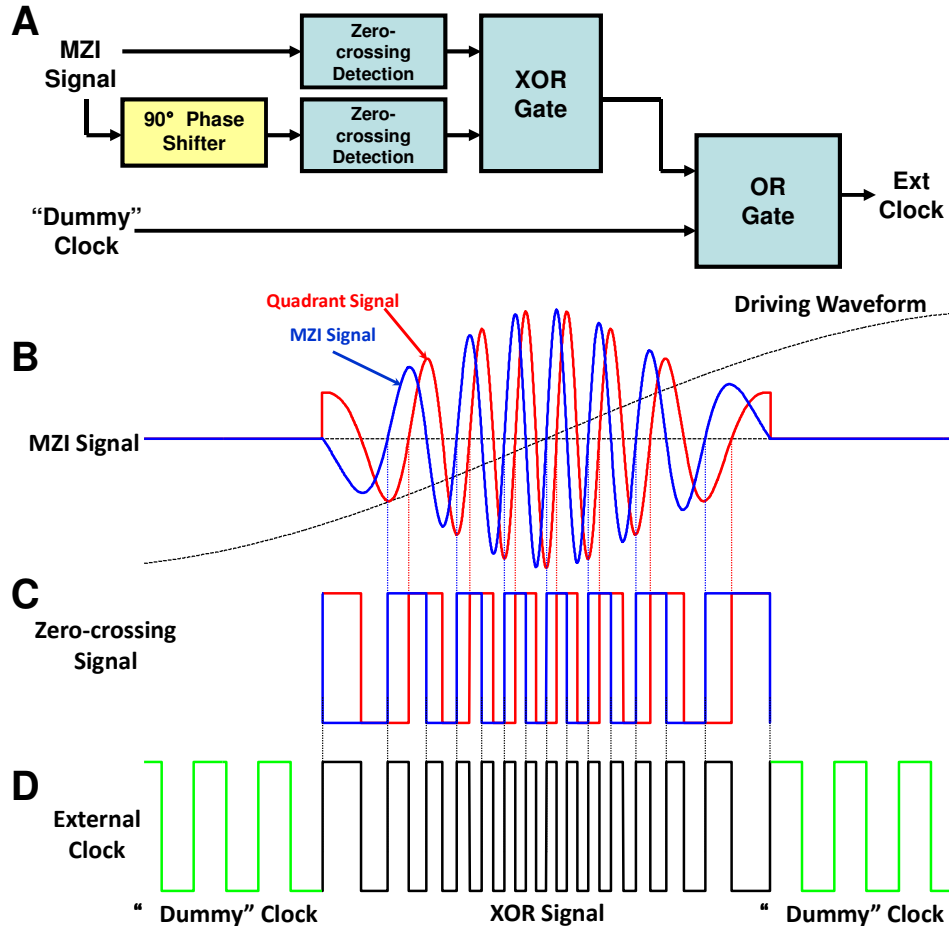


Fig. 1. (A) Schematic of external clock generator. (B) Illustration of the original MZI signal (blue line) and its quadrant signal after the broadband 90° phase shifter (red line). (C) Illustration of zero-crossing signals generated from the MZI and quadrant signals in (B). (D) External clock signal that combines the XOR gate output with a gap-filling dummy clock. The vertical dotted lines indicate the rising edges of the signals.

We will start with the basic considerations on designing the external clock signal for triggering the analog-to-digital converter (ADC) in a point-by-point fashion. In an SS-OCT system, a Mach-Zehnder interferometer (MZI) is generally used for generating the calibration signal. The commonly used numerical calibration algorithm uses the MZI signal to identify two data points on the OCT signal with equal K -spacing for every fringe cycle of the MZI calibration signal (e.g. the extrema or zero-crossing points). Under the Nyquist sampling theorem the imaging depth is thus the same as the optical path difference in the MZI. For the same reason, the new method requires two clock cycles with an equal K -space interval for each fringe cycle of the MZI calibration signal. The second design consideration is related to high-speed digitizer. Most high-speed, high resolution digitizers use an ADC with a pipeline

architecture that requires a clock duty cycle close to 50% to prevent the ADC from malfunctioning and prevent degradation of the spurious-free dynamic range (SFDR). Moreover, as most high-speed digitizers prefer to operate in a continuous mode in order to avoid repeated reset of internal circuitry (and the associated loss of speed), a dummy clock signal is thus needed to fill the idle gap between two consecutive OCT A-scans. Other two practical considerations are the propagation delay and jitter time of the external clock circuitry. Since the optical frequency information is encoded in time in an SS-OCT system, the propagation delay time of the external clock relative to the OCT signal must be carefully calculated and compensated. In addition, the electronic jitter time also needs to be minimized to avoid random triggering of the ADC. Thus a high-speed logic gate with minimal jitter time becomes critical for generating a stable external clock signal.

With the above considerations in view, an external clock generator has been developed and the schematic is shown in Fig. 1A. In order to generate two clock cycles for each MZI fringe, a broadband 90° phase shifter (JSPQ-65W + from Mini-Circuits) is employed to produce a quadrant signal from the original MZI calibration signal. The original and quadrant signals (Fig. 1B) are sent to two separate zero-crossing detection devices (MAX9693 from Maxim Integrated Products, Inc.) (Fig. 1A), which output two square-waves with “level high” corresponding to the positive portion of the original and the quadrant signal, respectively (Fig. 1C). The two square waves are then combined through an exclusive OR (XOR) gate (MC100EL07 from ON Semiconductor), which generates an external clock pulse when the two square waves overlap (Fig. 1D). This method produces two clock pulses for each MZI fringe cycle. The combination of a quadrant phase shifter and an XOR gate ensures the external clocks have an $\sim 50\%$ duty cycle. For our current off-the-shelf simple phase shifter, the change in phase unbalance over more than 3 octaves (5 MHz to 65 MHz) is less than 2° , and the resulted duty cycle only varies around $50\% \pm 0.3\%$, which helps maintain and maximize the SFDR of an ADC during the entire A-scan. As a result, the designed circuitry can generate a clock signal for A-scan rates from 20 to 100 kHz. To fill the empty gap on the external clock between adjacent A-scans, a dummy clock signal (the pulses in green color in Fig. 1D) is generated within the time duration complementary to the time gate for the zero-crossing detection, and then combined with the zero-crossing clock signal by an OR gate to form a final external clock (both the green and black pulses in Fig. 1D), which triggers a high-speed ADC by rising edges for uninterruptedly digitization point by point.

2.2 Swept-source OCT imaging system implemented with the real-time uniform K-space sampling method

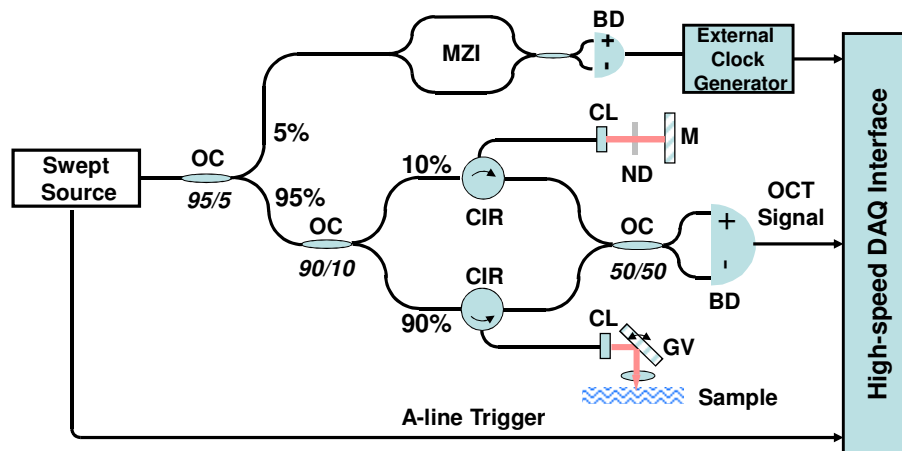


Fig. 2. Schematic of a swept-source OCT imaging system equipped with the real-time linear K-space sampling method. BD: balanced detector; CIR: circulator; CL: collimating lens; DAQ: data acquisition; GV: galvanometer mirror; M: mirror; ND: neutral density filter; OC: optical coupler.

The schematic of an SS-OCT system capable of real-time uniform K-space sampling is shown in Fig. 2. 5% of the output power from an FDML is sent to the MZI where the fringe signal is detected by a dual-balanced photo detector for external clock generation. The rest 95% of the laser output is launched into the OCT interferometer for imaging. The FDML operates at a scanning rate of 40 kHz (where only the forward scans were used for imaging). 90% of the optical power in the OCT interferometer is delivered to the sample arm and 10% is fed into the reference arm where a neutral density filter is used to further attenuate the reflected light intensity to avoid detector saturation. Two circulators are used to redirect the light from both the sample and reference arms to a 50:50 wideband optical coupler. The interference signal from the OCT interferometer is detected by another dual-balanced detector, from which the signal is acquired by a high-speed, 16-bit-resolution digitizer (ATS9462 from Alazartech Technologies Inc.) operating at the fast external clock mode.

3. Performance of real-time linear K-space sampling method

In our SS-OCT system, the free spectral range (FSR) of the MZI is set at 30 GHz, corresponding to an imaging depth of 2.5 mm (free space). Figure 3A shows the MZI interference signal during forward wavelength scanning with a 40 kHz sinusoidal driving waveform applied to the FFP-TF. The total number of fringe cycles of the forward scan signal is 409 and the corresponding number of the sampled data points per A-scan is therefore 818. It is noted that the frequency of the MZI signal varies a lot, e.g., the frequency of the slow fringe region (~25 MHz) with a zoomed-in version shown in the upper inset of Fig. 3A is less than half of the fast fringe region (~55 MHz) with a zoomed-in version shown in the lower inset. The external clock signal is shown in Fig. 3B which was to trigger the high-speed digitizer in a point by point fashion. The trigger frequency in the middle portion of the clock signal is about 110 MHz, while the clock frequency slows down to about 50 MHz at the edge of each A-scan. The frequency of the “dummy” clock should be high enough to fill in enough clock cycles in order to keep the digitizer working continuously, and in our case it was chosen to be 28 MHz or higher. It should be noted that the duty ratio of the external clock over the entire A-scan is close to 50% as shown in the insets in Fig. 3B, which is required for maintaining a good FSDR for a high-speed digitizer as mentioned previously.

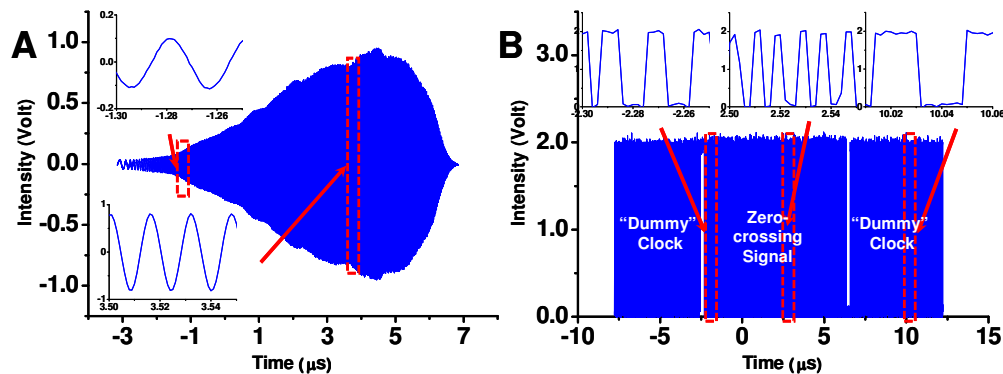


Fig. 3. (A) MZI interference signal. The upper and lower insets show the MZI signal at the beginning (or end) and the center of an A-scan, respectively, indicating that the MZI signal frequency varies during wavelength scanning. (B) External clock signal during forward wavelength scanning with the FFP-TF driven by a 40 kHz sinusoidal wave. The insets show the duty ratio of the external clock keeps very close to 50% which is essential to keep the high-speed digitizer working properly and continuously.

The measured axial resolution is ~9.3 μm in air as shown in Fig. 4A for a FDML laser of a 130-nm FWHM at a center wavelength 1310 nm (measured by an optical spectrum analyzer), and the axial resolution remains almost the same throughout the entire imaging depth of 2.5 mm (Fig. 4B). The measured detection sensitivity was greater than 120dB at the imaging depth of 1.0 mm.

One attractive advantage of the real-time linear K-space sampling method is the reduced requirement for the speed of data digitization, processing and storage by at least a factor of 2.5. Only 2 data points need to be digitized per MZI fringe cycle with the new method while at least 5 data points per cycle need to be digitized when using the conventional numerical calibration method. With our current hardware implementation, only about 800 points per A-scan need to be digitized as opposed to 2048 points per A-scan required by the conventional numerical calibration algorithm. Consequently, the new calibration method enables a digitizer of a given speed to handle a higher A-scan rate. Or equivalently, the new method can also handle a broader wavelength sweeping range and thus a light source of a broader spectrum bandwidth can be used in an SS-OCT system to achieve a better axial resolution. Furthermore, a higher A-scan rate can be supported with data acquisition, transfer, processing, display and storage performed in real time. Our current hardware can support an A-scan rate up to $\sim 100,000$ A-scans/sec with real-time linear K-space sampling without any interruption of data acquisition, transfer, processing or storage. In comparison, the conventional numerical calibration algorithm could only support up to $\sim 10,000$ A-scan/sec with spline interpolation or up to $\sim 50,000$ A-scans/sec with nearest neighbor interpolation. More importantly, our hardware-based real-time linear K-space sampling method provides a universal solution for an SS-OCT system with any A-scan rates provided that the clock signal is within the working frequency range of the clock-generation circuit, e.g. our prototype can handle an A-scan rate from 20 to 100 kHz without any adjustment. It is also noted that, unlike the numerical calibration algorithm which normally obtains the MZI calibration signal only once at the beginning (or the end) of OCT imaging and is thus sensitive to any instability or drifting of the laser spectrum and the FFP-TF scanning, the new calibration algorithm permits OCT interferometric fringes to be digitized against the corresponding real-time MZI calibration signal for all A-scans at all time. Table 1 summarizes the major improvements of the linear K-space sampling method over numerical calibration.

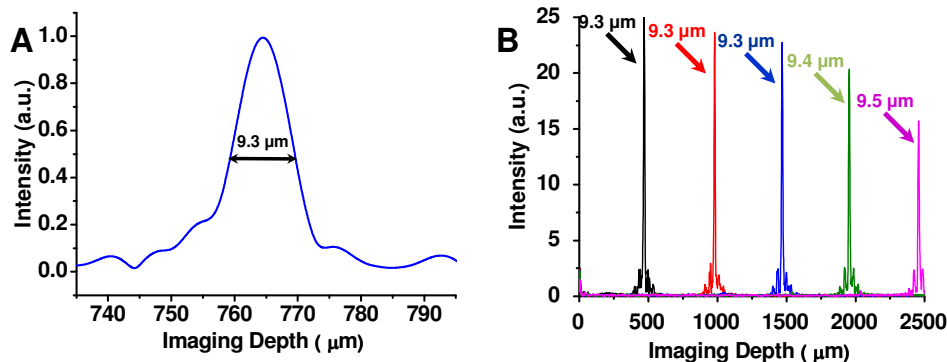


Fig. 4. (A) Point-spread function of an FDML-based SS-OCT system equipped with the real-time linear K-space sampling method. (B) Point-spread function versus imaging depth revealing no axial resolution degradation throughout the imaging depth of 2.5 mm.

Table 1. Comparison between real-time linear K-space sampling and numerical calibration

	Numerical Calibration	Linear-K Sampling
Acquired number of data points per A-line	2048	818
Calibrated data points number per A-line	680~750	818
Axial resolution (in air)	$\sim 10.2 \mu\text{m}$	$\sim 9.3 \mu\text{m}$
Data processing speed	$\sim 10,000$ A-line/sec (spline) $\sim 50,000$ A-lines/sec (nearest neighbor)	$\sim 100,000$ A-line/sec (no interpolation)
Data transfer and saving requirement	> 300 MB/sec	< 125 MB/sec

4. OCT imaging with real-time linear K-space sampling

The performance of the real-time linear K-space sampling method in an FDML-based SS-OCT system was demonstrated by imaging human finger tip and nail fold. The imaging beam was delivered to and scanned over the tissue with a handheld probe. The raw data of each A-scan of about 818 points are processed in real time via 4096 points fast Fourier transform after zero-padding, and the transformed A-scan size is 2048 pixels corresponding to an optical path of 2.5 mm. Representative OCT images are shown in Fig. 5. Both images have been rescaled along the depth direction by the average tissue index of refraction (i.e. ~ 1.4). The final image size is about 1024 x 1700 pixels corresponding to a physical dimension of 2 x 1.4 mm (lateral x depth). Structures such as sweat duct (SD), stratum corneum (SC), epidermis (E), nail fold (NF), and nail root (NR) can be clearly identified.

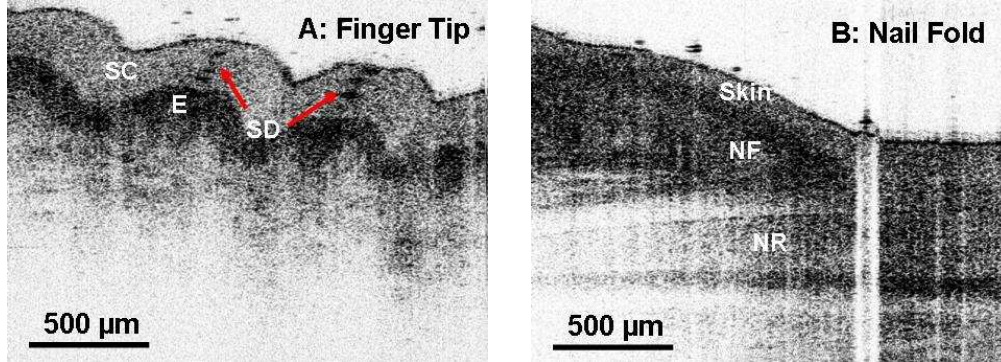


Fig. 5. Representative images acquired with an FDML-based SS-OCT system equipped with the real-time linear K-space sampling method. (A) Finger tip. (B) Finger nail fold.

5. Conclusion

In summary, a real-time linear K-space sampling method for a high-speed SS-OCT system was developed and demonstrated by incorporating an external clock generator with a uniform k-space distribution for triggering the digitizer in a point by point fashion. This method is relatively easy to implement since most of current high-speed digitizers support external clock mode with a varying frequency. It reduces the speed demand in OCT signal digitization, data transfer, processing and real-time saving. Owing to the property of the real-time uniform sampling, this method in principle may provide a better phase stability. Furthermore the new method supports a broad A-scan rate (20 to 100 kHz) without the need for a more expensive high-speed data acquisition system. The new method also affords a broader wavelength scanning range for achieving better axial resolution. The performance of the real-time linear K-space sampling method which was implemented in a FDML-based SS OCT system was demonstrated by imaging human tissues.

Acknowledgement

The authors are grateful to Alazar Inc. for providing the high-speed digitizer. This work was supported in part by the National Institutes of Health (NIH) (R21 CA116442, R01 CA120480 and 1R01 EB007636) and the National Science Foundation (NSF) Career Award (XDL).